metals

Article

Effect of Dispersing In Situ Al-Cu Intermetallic Compounds on Joint Strength in Friction Stir Welding of AA3003-H18 Sheets

Behrouz Abnar and Mousa Javidani *

Department of Applied Science, University of Quebec at Chicoutimi, Saguenay, QC G7H 2B1, Canada
* Correspondence: mjavidan@uqac.ca

Abstract: In this study, friction stir welding (FSW) was employed to join AA3003-H18 sheets by incorporating in situ Al-Cu intermetallic compounds within the stir zone. The FSW process was carried out under three distinct conditions: (I) without applying powder, (II) by introducing Cu powder, and (III) by incorporating Cu-Al mixed powder (50 vol.% Cu, 50 vol.% Al). The powder was embedded into the gap between two sheets. Subsequently, two-pass FSW, involving both forward and backward movements, was conducted with a rotational speed of 1200 rpm and traverse speed of 100 mm/min across all three experimental conditions. In the second and third conditions, the formation of in situ intermetallic compounds occurred through a solid-state reaction between Cu particles and Al within the stir zone. Examination of the stir zone through optical and electron microscopic studies revealed that the utilization of Cu-Al mixed powder resulted in finer and more uniformly distributed Cu clusters and Al-Cu intermetallics than samples welded with Cu powder alone. Notably, the stir zone of samples incorporating Cu-Al mixed powder exhibited finely dispersed, completely gray Al-Cu intermetallic particles, whereas those with only Cu powder displayed predominantly coarse core-shell particles in the microstructure. The introduction of Cu-Al mixed powder during FSW resulted in a stir zone with an average hardness of 74 HB, showing a 14% increase compared to the cases where Cu powder alone was added (65 HB). Tensile tests, conducted in both transverse and longitudinal directions on the FSWed samples, did not exhibit a consistent trend across the three mentioned conditions. Transverse tensile strength consistently ranged between 107 and 110 MPa, with joint efficiency varying from 52% to 54%. However, the longitudinal tensile strength of the joint with added Cu-Al mixed powder (158 MPa) surpassed those welded with Cu powder alone (134 MPa).

Keywords: friction stir welding; AA3003-H18; in situ intermetallic compounds; Cu-Al mixed powder; joint efficiency

Citation: Abnar, B.; Javidani, M. Effect of Dispersing In Situ Al-Cu Intermetallic Compounds on Joint Strength in Friction Stir Welding of AA3003-H18 Sheets. *Metals* **2024**, *14*, 277. https://doi.org/10.3390/met14030277

Academic Editor: Masahiro Fukumoto

Received: 1 February 2024
Revised: 23 February 2024
Accepted: 24 February 2024
Published: 27 February 2024

1. Introduction

Friction stir welding (FSW) is a solid-state technique used to join a variety of metallic materials. The most common application of the FSW is to join heat-treatable with non-heat-treatable Al alloys [1–3]. However, when applied to wrought non-heat-treatable Al alloys, FSW encounters unique challenges. The welding process induces recovery and dynamic recrystallization phenomena within the weld area, stemming from the heat input. Subsequently, the mechanical properties of the FSWed joints experience substantial decline in various zones, including the heat-affected zone (HAZ), thermomechanical-affected zone (TMAZ), and stir zone (SZ) [4–8].

Non-heat-treatable Al alloys (e.g., 1xxx, 3xxx, 4xxx, and 5xxx Series Alloys) exhibit limited responsiveness to heat treatment methods for improving the mechanical properties of the weld area [9,10]. Various approaches have been explored to address this challenge, with a primary focus on optimizing welding parameters such as tool rotational and traverse speeds, tool design, plunge depth, and tilt angle [4,6,11]. Additionally, alternative techniques, such as underwater FSW or water spray systems, have been employed to mitigate the loss of strength [12–15]. These interventions are predominantly employed to prevent the softening effect within the HAZ of defect-free weld metal [3,16–19].

To fortify the stir zone, a novel and effective strategy has been developed, involving the incorporation of reinforcement particles into the microstructure of non-heat-treatable Al alloys [11]. Mirjavadi et al. [20] has successfully utilized TiO_2 nanoparticles in AA5083 FSWed joints to increase the tensile strength of the weld. Similarly, Srivastava et al. [21] applied SiC nanoparticles during the FSW of AA5059, resulting in an ultimate tensile strength of the joint reaching to 342 MPa, surpassing the base metal strength of 321 MPa.

Reinforcement particles can be the intermetallic compounds formed by the in situ reaction between an aluminum matrix and metal powder [22]. This phenomenon was predominantly observed during friction stir processing (FSP). FSP has gained widespread application in the fabrication of Al matrix surface composites through the incorporation of reinforcement particles. In a study by Khodabakhsh et al. [23], Al_3Ti and MgO nanoparticles were formed in situ within the Al matrix of AA5052 when FSP was conducted by using TiO_2. Moreover, investigations into FSP of Al alloys with Cu powder revealed the formation of intermetallic compounds such as Al_2Cu, Al_2Cu_3, Al_4Cu_9, and AlCu [24–27].

The general applications of 3xxx series alloys include fuel tanks, chemical equipment, containers, cabinets, freezer liners, pressure vessels, storage tanks, and vehicles such as trucks and trailers [9], where the FSW process can be applied. In this study, the base material chosen was the work-hardened AA3003-H18 alloy. The experimental setup involved placing Cu powder and Cu-Al mixed powder in the gap between two sheets. The primary objective was to conduct a comprehensive analysis of the microstructural features of the stir zone and evaluate the mechanical properties of FSWed joints in both transverse and longitudinal directions. The formation of the Al-Cu intermetallic compounds was examined using different characterization techniques. Mechanical properties of the prepared specimens, encompassing longitudinal and transverse tensile properties as well as microhardness, were thoroughly investigated. Furthermore, the impact of intermetallic compounds on both transverse and longitudinal tensile strength was elucidated.

2. Experimental Procedure

In this study, as-received AA3003-H18 (Al–Mn alloy) sheets with a nominal chemical composition of Al-1.0Mn-0.35Fe-0.22Si-0.06Cu (wt.%) were used as the base metal. Copper powder with a particle size of $\leq$20 μm and a purity of $\geq$99.0% was used in the research. Additionally, Al powder with a particle size of $\leq$44 μm and a purity of $\geq$99.0% was incorporated to form a mixture of Al and Cu powder.

Friction stir welding of the sheets was conducted using a rotational tool made by H13 tool steel. The tool specifications included a shoulder diameter of 20 mm, a cylindrical pin diameter of 5 mm, and a pin height of 2.8 mm. The tool tilt angle relative to the workpiece surface was set at 2.5 degrees from the vertical axis during the weld process.

The FSW process was applied to samples with the dimension of 100 mm$\times$ 50 mm$\times$ 3 mm under three specified conditions outlined in Table 1. In the case of samples II and III, a gap was deliberately introduced between two sheets, and this was subsequently filled with Cu and a mixture of Cu-Al powder, respectively. For all cases, FSW consisted of two passes, with the second pass moving in the opposite direction of the first pass. Figure 1 provides a schematic representation of the FSW process, illustrating the addition of powder into the gap between two sheets.

To evaluate mechanical properties, both longitudinal and transverse tensile samples were machined according to ASTM E8M [28] with a gauge length of 32 mm. In the transverse tensile test specimens, indicated in Figure 2a, the stir zone was placed at the center of the gauge length. On the other hand, in the longitudinal tensile test (Figure 2b), samples were oriented parallel to the travel direction to ensure that the entire gauge length was composed of stir zone (SZ) material. Furthermore, Vickers microhardness tests were carried out along a transverse line across the cross-section of FSWed samples. The microhardness at the centerline of the cross-section, positioned at a depth of 1.5 mm from the surface, was determined employing Vickers microhardness equipment under a load of 100 g for a duration of 15 s.

Table 1. FSW conditions with applying metallic powder.

Sample No.	FSW Condition	Rotational Speed (rpm)	Traverse Speed (mm/min)	The Composition of the Powder Mixture	The Gap Size between Two Sheets (mm)
I	Without adding powder	1200	100	-	-
II	With adding Cu powder	1200	100	100% Cu	0.4
III	With adding Cu-Al mixed powder	1200	100	50 vol.% Cu, 50 vol.% Al (77 wt.% Cu, 23 wt.% Al)	0.4

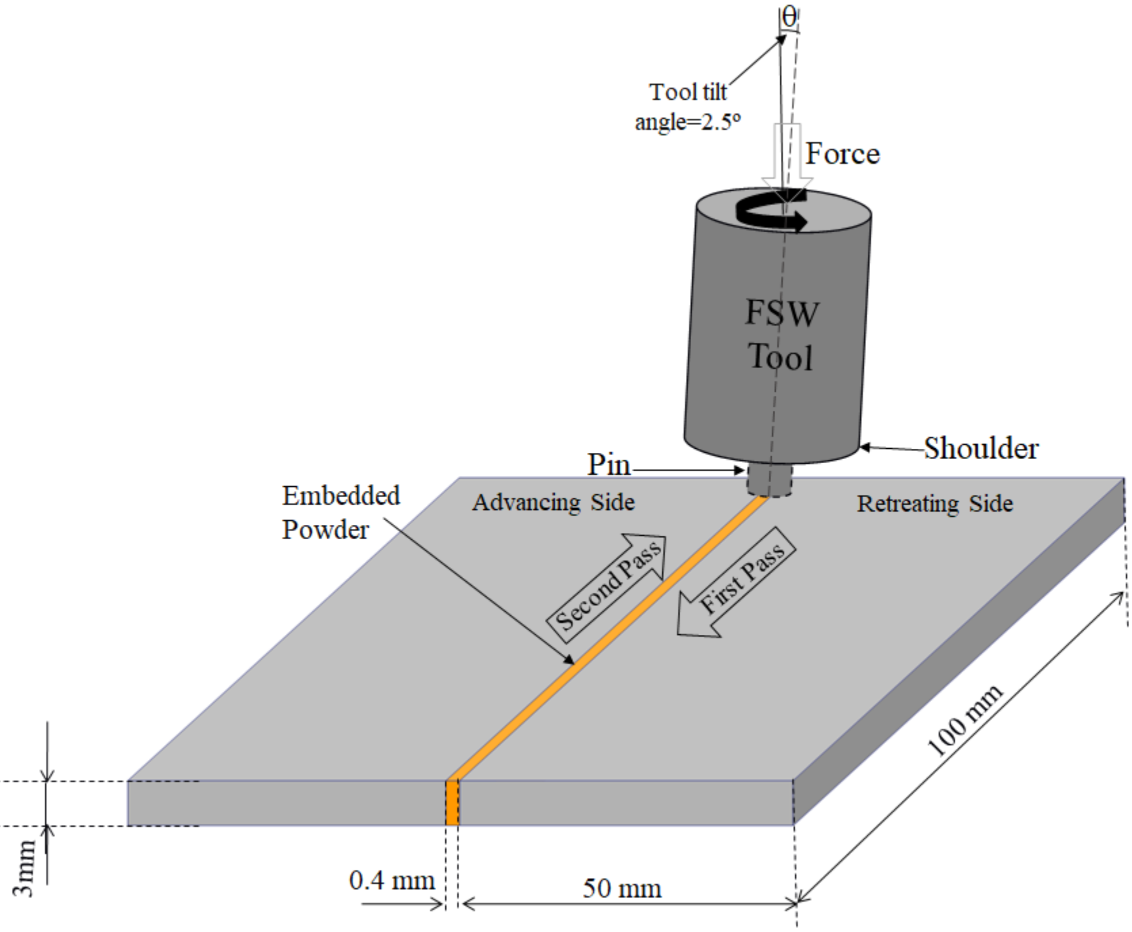

Figure 1. Schematic of FSW process with embedding powder.

The microstructural analysis of the stir zone in the FSWed samples was conducted on the cross-section of the weld, perpendicular to the FSW direction, and observed by optical microscopy (OM) after polishing. Additionally, the distribution of the compounds in this region was examined using the backscattered electron (BSE) detector in scanning electron microscopy (SEM). The identification of formed intermetallic compounds was carried out using energy dispersive spectroscopy (EDS).

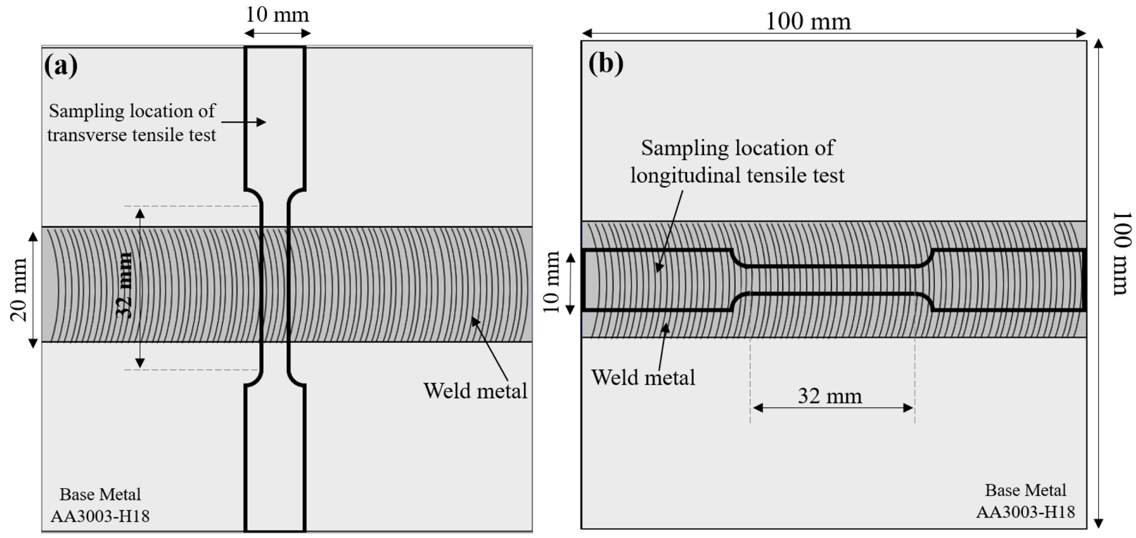

Figure 2. Schematic of sampling location of (**a**) transverse and (**b**) longitudinal tensile tests.

3. Result and Discussion

3.1. Microstructure

Figure 3 shows the stir zone microstructure for the three conditions outlined in Table 1. In the case of sample No. I, where no metal powder was used in the FSW process, the microvoids (<2 µm), attributed to the material stirring or material flow [29], were uniformly observed in the stir zone, as shown in Figure 3a. The optical micrographs captured in the second and third condition (sample II and III), are presented in Figure 3b,c, respectively. These images reveal clusters of the Cu particles and formed Al-Cu intermetallic compounds dispersed within the stir zone. It is evident that not all Cu powder transformed into reinforced particles; some remained in its original Cu form. As seen in the optical microscopy images, the particles exhibited distinct layers, a characteristic further discussed with SEM-EDS results. The comparison of the stir zone microstructure of sample II and III reveals a significant refined and more uniform distribution of particles after the introduction of Cu-Al mixed powder. The size distribution of Cu/Al-Cu intermetallic particles in Figure 4 indicates that the predominant particle size range in sample II was between 10 and 20 µm, whereas a higher fraction of particles with sizes less than 10 µm was observed in sample III. During FSW, the metal powder was compressed by the tool's shoulder in the gap between two sheets right before being stirred into the seam. Applying only Cu powder led to the formation of a large Cu cluster due to the cold-welding mechanism. The strong direct contact between particles induced cold welding under pressure, enlarging the cluster size [30,31]. When mixed Cu and Al powder were used, the contact between Cu particles was limited, because Cu particles were surrounded by Al particles. The incorporation of Cu-Al mixed powder effectively reduced cold welding between Cu powder particles, prevented agglomeration, and inhibited the formation of large Cu clusters after the FSW process.

In addition to ensuring uniform reinforcement dispersion, the effective formation of in situ intermetallics significantly influences the mechanical properties of the stir zone. Therefore, a comprehensive examination of the various compounds formed in the microstructure due to the presence of Cu particles is essential. Figure 5a–c presents the SEM-BSE micrographs of the stir zone in FSWed samples I, II, and III, respectively. Consistent with the optical micrographs, microvoids are evident in the sample without the addition of metal powder, as shown in Figure 5a. Furthermore, Figure 5b,c reveals two distinct types of particles within the microstructure of the stir zone in FSWed samples II and III. These include the coarse core-shell structured particles and the fine, completely gray particles, each exhibiting varying quantities within samples II and III. A comparison of Figure 5b and c reveals a significant reduction in the proportion of unreacted Cu in the inner part of the core-shell structured particles when a mixture of Al and Cu powder is utilized. In sample III, powder particles were clustered into smaller sizes within the stir zone, promoting direct contact between a greater number of small-sized Cu particles and the Al matrix [32]. This clustering effect facilitates faster heat transfer to the core of the small clusters during FSW, expediting the formation of intermetallic compounds. Another notable outcome of employing Cu-Al mixed powder is the presence of fractured Al-Cu intermetallics, as depicted in Figure 5c, contributing to a uniform distribution of in situ compounds within the Al matrix.

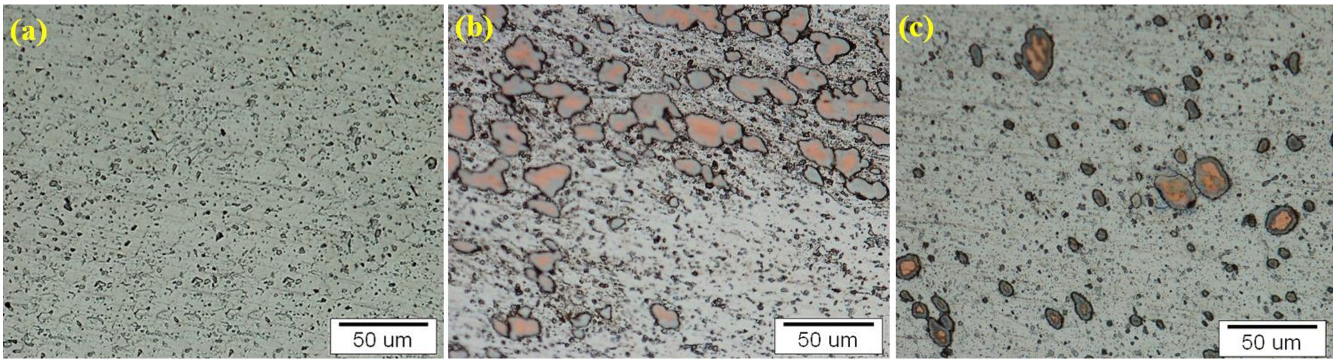

Figure 3. Optical microscope images of the stir zone microstructure: (**a**) without adding powder, (**b**) with adding Cu powder, (**c**) with adding Cu-Al mixed powder.

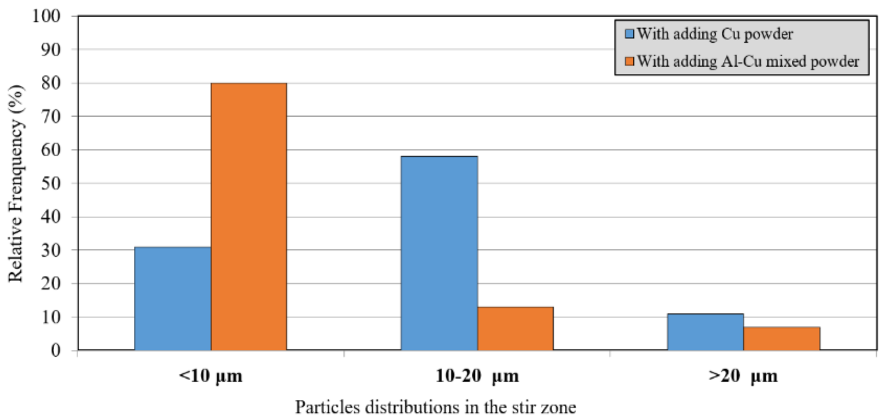

Figure 4. Size distribution of Cu/Al-Cu intermetallics particles in the stir zone microstructure of FSWed samples produced using Cu powder vs. Cu-Al mixed powder.

In Figure 5d, elemental mapping conducted with EDS analysis reveals four distinct types of Cu-containing compounds corresponding to those shown in Figure 5e. The results indicate that each layer of the core-shell structured particles comprises a unique stoichiometric composition, extending from the core to the Al matrix. The concentration of elemental Al decreases from the Al matrix side to the core, while the concentration distribution of elemental Cu exhibits the opposite trend. The observed color variations between layers can be attributed to differences in atomic weight resulting from distinct stoichiometric composition [27].

Referring to the Al-Cu binary alloy phase diagram presented in Figure 6, and considering the typical temperature range of the stir zone during FSW of Al alloys (<500 °C) [3], six potential intermetallic phases can form in the Al-Cu system within the stir zone: Al_2Cu (θ), AlCu (η_2), Al_3Cu_4 (ζ_2), Al_2Cu_3 (δ), Al_4Cu_9 (γ_1), and $AlCu_4$ (α_2) [22,32–34]. The formation of any of these intermetallic phases primarily depends on the concentration of Cu/Al and the dominant temperature within the stir zone [32]. By employing the EDS technique, which provides semi-quantitative results, we made predictions regarding the compounds' formation. The layers of the core-shell structured particles consist of unreacted Cu, Al_4Cu_9

(γ_1), and Al_3Cu_4 (ζ_2), corresponding to zones A, B, and C in Figure 5e, respectively. Additionally, the finely dispersed, entirely gray particles in zone D exhibit an analysis consistent with Al_2Cu (θ). Notably, as the layer approaches the center of the core-shell structured particles, the concentration of Cu in the intermetallic phase increases.

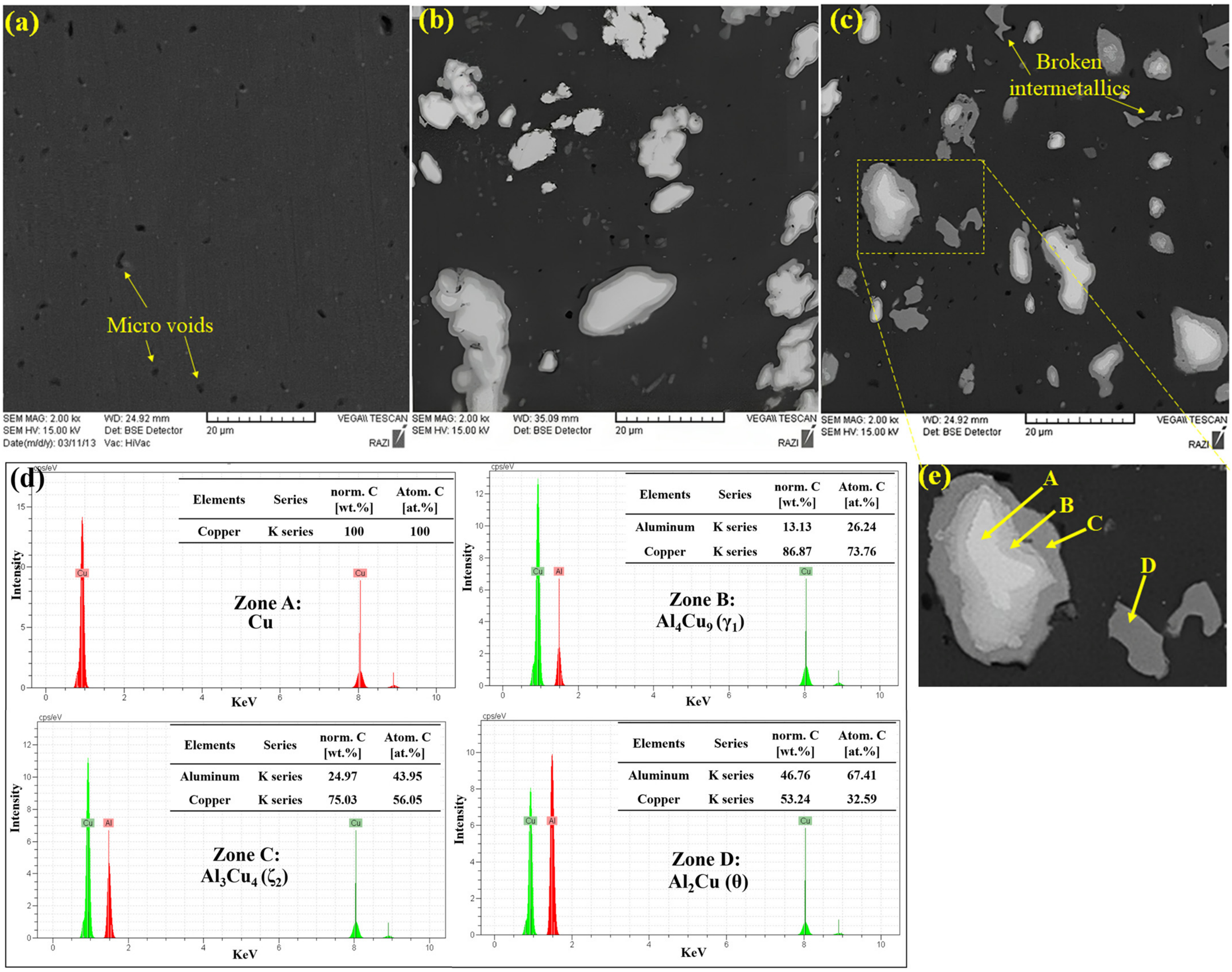

Figure 5. BSE-SEM micrographs of the stir zone: (**a**) without adding powder, (**b**) with adding Cu powder, (**c**) with adding Cu-Al mixed powder; (**d**) EDS results of the marked point A, B, C, and D in (**e**) enlarged view of the rectangle in "c".

Additionally, the increased darkness observed in the SEM image corresponds to a higher concentration of Al within the layers. The well-defined bright region at the core signifies unreacted Cu, predominantly observed in particles with diameters exceeding 10 µm. Throughout the FSW process, the Cu powder particles, experiencing intense heat input and plastic deformation, undergo enrichment with Al atoms through interplanar diffusion–interfacial migration effects. Consequently, this leads to the formation of distinct layers with varying stoichiometric compositions [22,27].

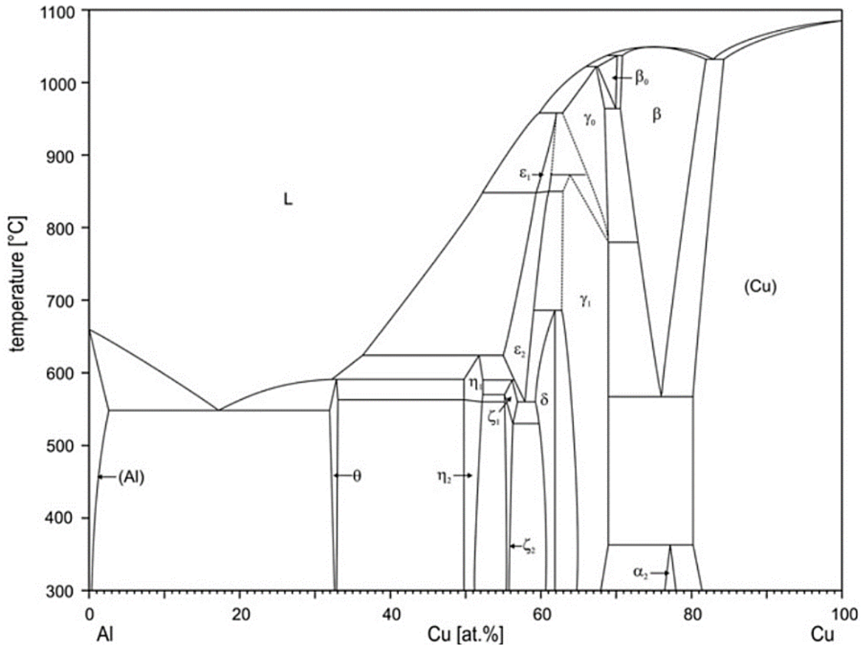

Figure 6. Phase diagram of Al-Cu binary alloy system. Reprinted with permission from ref. [33]. Copyright 2024 Elsevier.

3.2. Mechanical Properties

To assess the influence of utilizing both Cu powder and Cu-Al mixed powder on the mechanical properties of the FSW samples, we conducted comprehensive evaluations using microhardness measurements, as well as longitudinal and transverse tensile tests. In Figure 7, the microhardness profile across various zones of three FSWed samples is depicted. In the case of FSW of AA3003-H18 sheets without adding metal powder (sample No. I), it is evident that the hardness in the weld area, including HAZ, TMAZ, and SZ, is approximately 25% lower than that of the base metal. This reduction is attributed to the activation of the softening mechanisms, including recrystallization and recovery in the weld area [16,35]. The decrease in hardness in the weld zone of FSWed samples, compared to the base metal, can primarily be ascribed to three factors: (1) the static recrystallization of the HAZ induced by annealing, (2) dynamic recrystallization of the SZ resulting from hot deformation, and (3) the dynamically recovered subgrain structure in the non-recrystallized TMAZ [16].

In Figure 7, a noteworthy elevation in the average microhardness of the stir zone is evident upon the incorporation of Cu powder and Cu-Al mixed powder. This increase in hardness is attributed to the high hardness characteristics of the formed intermetallic compounds within the matrix [26,36]. Specifically, the average hardness in the stir zone measured 34, 65, and 74 HV for samples I, II, and III, respectively. In samples II and III, the average hardness surpassed that of the base metal by approximately 38% and 57%, respectively. The incorporation of Cu-Al mixed powder in the FSW process of AA3003-H18 sheets led to a 14% higher average hardness in the stir zone, demonstrating reduced fluctuations compared to cases where only Cu powder was employed. Microstructure characterization revealed a more uniform distribution of particles and a higher fraction of intermetallics, particularly Al-Cu in situ intermetallic compounds, when Cu-Al mixed powder was used. In contrast, in sample II where only Cu powder was employed, the majority of the coarse core-shell structured particles consisted of unreacted Cu. This composition adversely affected the hardness value and resulted in more significant fluctuations in hardness.

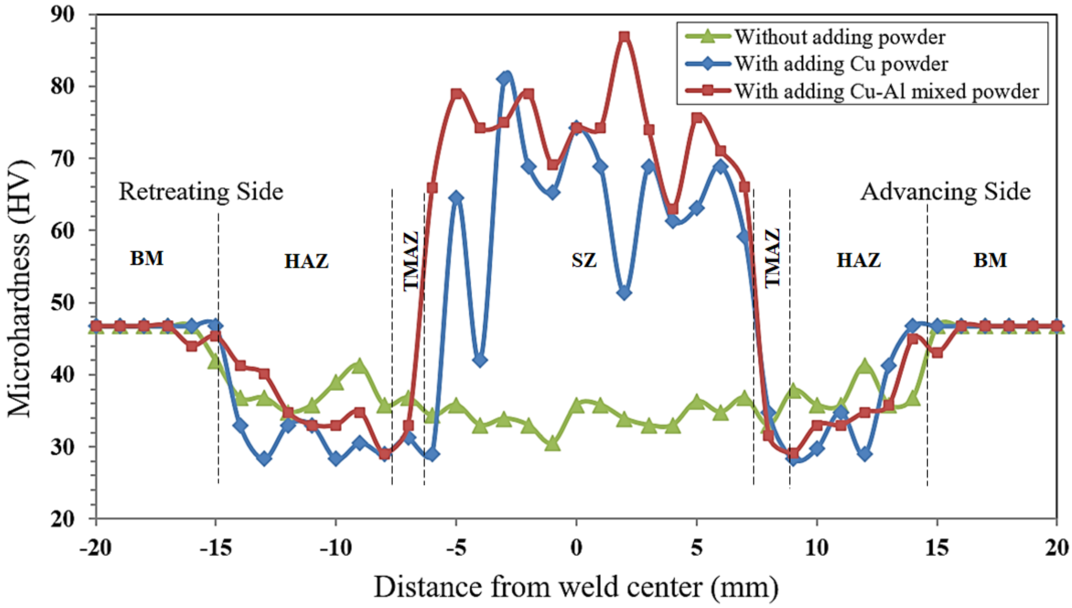

Figure 7. Hardness distribution in the cross-section of the welded joint without and with adding powder.

The stress–strain curves presented in Figure 8 illustrate the results from both longitudinal and transverse tensile tests conducted on samples No. I, II, and II. The results of both longitudinal and transverse tensile tests, including ultimate tensile strength (UTS), yield strength, and elongation have been provided in Table 2 for the three designated samples. As shown in Figure 8, the transverse tensile properties samples—specifically UTS and yield strength—exhibited remarkable similarity among the three samples, showing no discernible variations. Figure 9 shows the fracture locations of the welded specimens after the transverse tensile test. For all three studied samples, the failure location is located in the HAZ region. Notably, the strength in transverse tensile tests for all three samples was influenced by the HAZ, identified as the weakest region through hardness assessments. As a result, the fractures in all transverse tensile test samples occurred within the HAZ. Given the uniformity in the FSW process parameters for samples No. I, II, and II, and the consequent equal heat input to the HAZ area across these specimens, similarities emerged in microstructure evolution and mechanical properties within the HAZ. This uniformity led to the attainment of identical transverse tensile properties among the samples. Despite the attempts to enhance the transverse mechanical properties by introducing in situ Al-Cu intermetallics in the stir zone, such interventions were found to be ineffective in improving the overall performance of the FSWed samples. The longitudinal tensile test samples, extracted from the reinforced stir zone as shown in Figure 2b, indicated an evident increase in strength when Cu powder and Cu-Al mixed powder were incorporated. In the longitudinal tensile test of sample II, the UTS indicated an approximate 20% surge compared to sample I. Furthermore, the introduction of Cu-Al mixed powder further enhanced the UTS, marking a notable increase of around 42% relative to sample I. These longitudinal tensile test samples can be classified as aluminum matrix composite (AMC) reinforced by in situ Al-Cu intermetallics. Prior research has successfully employed FSP to develop the surface AMC with distributed Al-Cu intermetallics in various studies [22,32,37]. The Al-Cu intermetallic particles distributed within the Al matrix can significantly contribute to strengthening through the Orowan mechanism. Orowan strengthening arises from the impediment posed by closely spaced hard particles to the movement of dislocations [22,38]. Furthermore, a high density of dislocations is induced by the difference in coefficients of thermal expansion (CTE) between the matrix and reinforcing particles. This, in turn, restricts plastic deformation, ultimately leading to a substantial improvement in strength [22].

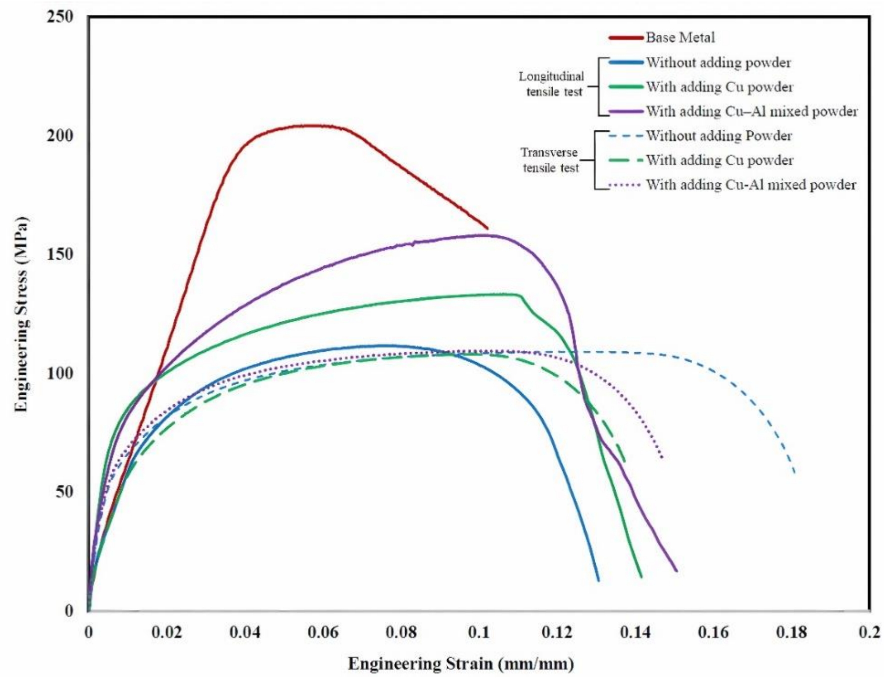

Figure 8. Stress–strain curves of the tensile test specimens. Solid lines represent longitudinal tensile tests, while dashed lines represent transverse tensile tests. The base metal curve shows the tensile strength of the AA3003-H18 without welding.

Table 2. Tensile strength, yield strength, and elongation of the welded joint without and with adding powder.

Tensile Properties	Ultimate Tensile Strength (MPa)			Yield Strength (MPa)			Elongation (%)		
Sample No.	**I**	**II**	**III**	**I**	**II**	**III**	**I**	**II**	**III**
Transverse Tensile test	110	107	109	73	75	76	18	14	15
Longitudinal Tensile test	111	134	158	71	85	85	13	14	15

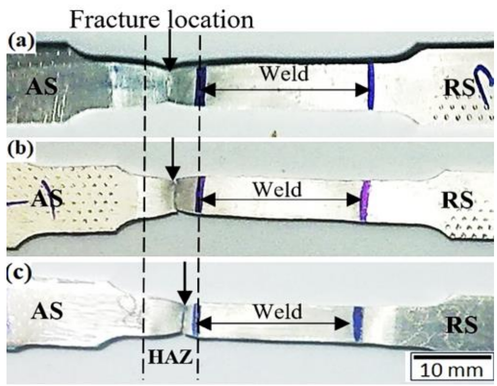

Figure 9. Fracture locations after transverse tensile tests of the FSWed specimens: (**a**) without adding powder, (**b**) with adding Cu powder, (**c**) with adding Cu-Al mixed powder.

As indicated in Table 2, the substitution of Cu-Al mixed powder with Cu powder led to a notable increase of ~18% in UTS, elevating it from 134 MPa to 158 MPa. This enhancement was attributed to the finer in situ Al-Cu intermetallic compounds and their uniform distribution, characterized by their close proximity to each other. The reduction in spacing between the reinforced particles within the matrix, achieved through a uniform dispersion, played a crucial role in significantly amplifying the strengthening effect through

Orowan mechanism [39]. This factor emerged as a key contributor to the superior strength observed in metal matrix composites produced by FSP [23,40].

It is important to note that the impact of the uniform distribution of the in situ intermetallic compounds was primarily evident in the longitudinal tensile strength. While the incorporation of Cu or Cu-Al powder exhibited positive effects on longitudinal tensile properties, it did not result in improvements in transverse tensile properties. From a welding perspective, assessing joint efficiency becomes essential for a more comprehensive evaluation of the effectiveness of adding metal powder. Joint efficiency in welding refers to the ratio of the strength of a welded joint to the strength of the base material. Expressed as a percentage, it serves as a metric for evaluating how effectively the welded joint can carry load in comparison to the original, unwelded material [41]. In general, transverse tensile strength is used to determine the joint efficiency of a weld [42,43]. Relative to the base metal tensile strength (204 MPa), the joint efficiency of sample No. II and III was measured at 52% to 54%, respectively. These values closely align with the joint efficiency observed in sample I, which did not incorporate any metal powder. As previously mentioned, the transverse tensile strength was influenced by the mechanical properties of HAZ, where reinforcement particles were not embedded. To enhance the transverse tensile strength and joint efficiency, implementing an efficient cooling system for the heat-affected zone (HAZ) should be considered. Cooling of HAZ, recognized as the weakest area, has been proved to be an effective technique for reducing the heat input during the FSW process, and subsequently increasing the strength of this region. Various cooling methods, such as water spray, compressed air, liquid nitrogen, Cu backing, or underwater FSW, can be employed for this purpose [12,15,44–46].

4. Conclusions

The investigation into the friction stir welding (FSW) of AA3003-H18 sheets, incorporating Cu powder and Cu-Al mixed powder in both forward and backward passes, has yielded significant insights. The key findings are outlined below:

- FSW with the addition of Cu-Al mixed powder led to a notably finer and more uniformly distributed array of in situ Al-Cu intermetallic compounds, as compared to joints welded by adding Cu powder alone.
- Two distinct particle types observed in the microstructure of FSWed samples using metal powder: coarse core-shell particles and fine, completely gray particles, comprising Al_4Cu_9 (γ_1), Al_3Cu_4 (ζ_2), and Al_2Cu (θ). The use of Cu-Al mixed powder promoted the formation of smaller clusters, reduced unreacted Cu, and induced the presence of broken Al-Cu intermetallics, resulting in an improved distribution.
- FSW with the addition of Cu-Al mixed powder exhibited an average hardness value of 74 HB in the stir zone, representing a 14% increase compared to joints welded with Cu powder alone (65 HB). This enhanced hardness can be attributed to the formation of high hardness intermetallic compounds within the matrix, initiating strengthening mechanisms.
- The FSWed joints incorporating Cu powder and Cu-Al mixed powder demonstrated superior longitudinal tensile strength compared to the samples without the addition of metal powder. This improvement can be ascribed to the heightened strengthening effect via the Orowan mechanism.
- While embedding Cu-Al mixed powder led to a higher longitudinal tensile strength relative to joints with added Cu powder, the transverse tensile strengths in both two conditions (adding Cu powder and Cu-Al mixed powder) were nearly identical, indicating similar joint efficiency. These results closely aligned with cases where welding was performed without the addition of metal powder.

In conclusion, the utilization of Cu-Al mixed powder in FSW of AA3003-H18 sheets has proven to be a promising strategy for enhancing microstructural characteristics, hardness, and tensile strength in the weld metal. These findings contribute valuable insights to the optimization of FSW processes for Al alloys.

Author Contributions: Methodology, B.A. and M.J.; validation, M.J.; formal analysis, B.A. and M.J.; investigation, B.A. and M.J.; writing—original draft, B.A.; writing—review and editing, M.J.; supervision, M.J. All authors have read and agreed to the published version of the manuscript.

Funding: This research received no external funding.

Data Availability Statement: The raw data supporting the conclusions of this article will be made available by the authors on request.

Acknowledgments: The authors wish to express their gratitude for the technical support and insightful discussions provided by the CIMTAL research group.

Conflicts of Interest: The authors declare no conflict of interest.

References

1. Mathers, G. *The Welding of Aluminium and Its Alloys*; Elsevier: Amsterdam, The Netherlands, 2002.
2. Rai, R.; De, A.; Bhadeshia, H.K.D.H.; DebRoy, T. Friction stir welding tools. *Sci. Technol. Weld. Join.* **2011**, *16*, 325–342. [CrossRef]
3. Mishra, R.S.; Ma, Z. Friction stir welding and processing. *Mater. Sci. Eng. R Rep.* **2005**, *50*, 1–78. [CrossRef]
4. Abnar, B.; Kazeminezhad, M.; Kokabi, A. Effects of heat input in friction stir welding on microstructure and mechanical properties of AA3003-H18 plates. *Trans. Nonferrous Met. Soc. China* **2015**, *25*, 2147–2155. [CrossRef]
5. Liu, H.; Fujii, H.; Maeda, M.; Nogi, K. Heterogeneity of mechanical properties of friction stir welded joints of 1050-H24 aluminum alloy. *J. Mater. Sci. Lett.* **2003**, *22*, 441–444. [CrossRef]
6. Liu, H.; Fujii, H.; Maeda, M.; Nogi, K. Mechanical properties of friction stir welded joints of 1050–H24 aluminium alloy. *Sci. Technol. Weld. Join.* **2003**, *8*, 450–454. [CrossRef]
7. Rao, D.; Huber, K.; Heerens, J.; Dos Santos, J.F.; Huber, N. Asymmetric mechanical properties and tensile behaviour prediction of aluminium alloy 5083 friction stir welding joints. *Mater. Sci. Eng. A* **2013**, *565*, 44–50. [CrossRef]
8. Peel, M.; Steuwer, A.; Preuss, M.; Withers, P.J. Microstructure, mechanical properties and residual stresses as a function of welding speed in aluminium AA5083 friction stir welds. *Acta Mater.* **2003**, *51*, 4791–4801. [CrossRef]
9. Davis, J.R. *Aluminum and Aluminum Alloys*; ASM International: Detroit, MI, USA, 1993.
10. Abnar, B.; Kazeminezhad, M.; Kokabi, A. The effect of Cu powder during friction stir welding on microstructure and mechanical properties of AA3003-H18. *Metall. Mater. Trans. A* **2014**, *45*, 3882–3891. [CrossRef]
11. Abnar, B.; Gashtiazar, S.; Javidani, M. Friction stir welding of non-heat treatable Al alloys: Challenges and improvements opportunities. *Crystals* **2023**, *13*, 576. [CrossRef]
12. Wang, B.; Chen, F.F.; Liu, F.; Wang, W.G.; Xue, P.; Ma, Z.Y. Enhanced mechanical properties of friction stir welded 5083Al-H19 joints with additional water cooling. *J. Mater. Sci. Technol.* **2017**, *33*, 1009–1014. [CrossRef]
13. Tan, Y.; Wang, X.M.; Ma, M.; Zhang, J.X.; Liu, W.C.; Fu, R.D.; Xiang, S. A study on microstructure and mechanical properties of AA 3003 aluminum alloy joints by underwater friction stir welding. *Mater. Charact.* **2017**, *127*, 41–52. [CrossRef]
14. Heirani, F.; Abbasi, A.; Ardestani, M. Effects of processing parameters on microstructure and mechanical behaviors of underwater friction stir welding of Al5083 alloy. *J. Manuf. Process.* **2017**, *25*, 77–84. [CrossRef]
15. Heidarzadeh, A.; Javidani, M.; Mofarrehi, M.; Farzaneh, A.; Chen, X.G. Submerged dissimilar friction stir welding of AA6061 and AA7075 aluminum alloys: Microstructure characterization and mechanical property. *J. Met.* **2021**, *10*, 1592. [CrossRef]
16. Threadgill, P.; Leonard, A.J.; Shercliff, H.R.; Withers, P.J. Friction stir welding of aluminium alloys. *Int. Mater. Rev.* **2009**, *54*, 49–93. [CrossRef]
17. Meng, X.; Huang, Y.; Cao, J.; Shen, J.; dos Santos, J.F. Recent progress on control strategies for inherent issues in friction stir welding. *Prog. Mater. Sci.* **2021**, *115*, 100706. [CrossRef]
18. Woo, W.; Balogh, L.; Ungár, T.; Choo, H.; Feng, Z. Grain structure and dislocation density measurements in a friction-stir welded aluminum alloy using X-ray peak profile analysis. *Mater. Sci. Eng. A* **2008**, *498*, 308–313. [CrossRef]
19. Yazdipour, A.; Aval, H.J. An investigation of the microstructures and properties of metal inert gas and friction stir welds in aluminum alloy 5083. *Sadhana* **2011**, *36*, 505–514. [CrossRef]
20. Mirjavadi, S.S.; Alipour, M.; Emamian, S.; Kord, S.; Hamouda, A.M.S.; Koppad, P.G.; Keshavamurthy, R. Influence of TiO_2 nanoparticles incorporation to friction stir welded 5083 aluminum alloy on the microstructure, mechanical properties and wear resistance. *J. Alloys Compd.* **2017**, *712*, 795–803. [CrossRef]
21. Srivastava, M.; Rathee, S. A study on the effect of incorporation of SiC particles during friction stir welding of Al 5059 alloy. *Silicon* **2021**, *13*, 2209–2219. [CrossRef]
22. Huang, G.; Hou, W.; Li, J.; Shen, Y. Development of surface composite based on Al-Cu system by friction stir processing: Evaluation of microstructure, formation mechanism and wear behavior. *Surf. Coat. Technol.* **2018**, *344*, 30–42. [CrossRef]
23. Khodabakhshi, F.; Simchi, A.; Kokabi, A.H.; Sadeghahmadi, M.; Gerlich, A.P. Reactive friction stir processing of AA 5052–TiO_2 nanocomposite: Process–microstructure–mechanical characteristics. *Mater. Sci. Technol.* **2015**, *31*, 426–435. [CrossRef]
24. Hsu, C.; Kao, P.; Ho, N. Ultrafine-grained Al–Al_2Cu composite produced in situ by friction stir processing. *Scr. Mater.* **2005**, *53*, 341–345. [CrossRef]

25. Inada, K.; Fujii, H.; Ji, Y.S.; Sun, Y.F.; Morisada, Y. Effect of gap on FSW joint formation and development of friction powder processing. *Sci. Technol. Weld. Join.* **2010**, *15*, 131–136. [CrossRef]
26. Zykova, A.; Chumaevskii, A.; Gusarova, A.; Kalashnikova, T.; Fortuna, S.; Savchenko, N.; Kolubaev, E.; Tarasov, S. Microstructure of in-situ friction stir processed Al-Cu transition zone. *Metals* **2020**, *10*, 818. [CrossRef]
27. Papantoniou, I.G.; Markopoulos, A.P.; Manolakos, D.E. A new approach in surface modification and surface hardening of aluminum alloys using friction stir process: Cu-reinforced AA5083. *Materials* **2020**, *13*, 1278. [CrossRef]
28. ASTM International. *E8/E8M-22: Standard Test Methods for Tension Testing of Metallic Materials*; ASTM International: West Conshohocken, PA, USA, 2022.
29. Padhy, G.; Wu, C.; Gao, S. Friction stir based welding and processing technologies-processes, parameters, microstructures and applications: A review. *J. Mater. Sci. Technol.* **2018**, *34*, 1–38. [CrossRef]
30. Hirayama, Y.; Suzuki, K.; Yamaguchi, W.; Takagi, K. Cold welding behavior of fine bare aluminum powders prepared by new low oxygen induction thermal plasma system. *J. Alloys Compd.* **2018**, *768*, 608–612. [CrossRef]
31. Dixit, M.; Srivastava, R. The effect of copper granules on interfacial bonding and properties of the copper-graphite composite prepared by flake powder metallurgy. *Adv. Powder Technol.* **2019**, *30*, 3067–3078. [CrossRef]
32. Mahmoud, E.R.; Al-qozaim, A.M. Fabrication of in-situ Al-Cu intermetallics on aluminum surface by friction stir processing. *Arab. J. Sci. Eng.* **2016**, *41*, 1757–1769. [CrossRef]
33. Ponweiser, N.; Lengauer, C.L.; Richter, K.W. Re-investigation of phase equilibria in the system Al-Cu and structural analysis of the high-temperature phase η1-Al1−δCu. *Intermetallics* **2011**, *19*, 1737–1746. [CrossRef] [PubMed]
34. Khajeh, R.; Jafarian, H.R.; Seyedein, S.H.; Jabraeili, R.; Eivani, A.R.; Park, N.; Kim, Y.; Heidarzadeh, A. Microstructure, mechanical and electrical properties of dissimilar friction stir welded 2024 aluminum alloy and copper joints. *J. Mater. Res. Technol.* **2021**, *14*, 1945–1957. [CrossRef]
35. Lohwasser, D.; Chen, Z. *Friction Stir Welding: From Basics to Applications*; Elsevier: Amsterdam, The Netherlands, 2009.
36. Azizieh, M.; Iranparast, D.; Dezfuli, M.A.G.; Balak, Z.; Kim, H.S. Fabrication of Al/Al_2Cu in situ nanocomposite via friction stir processing. *Trans. Nonferrous Met. Soc. China* **2017**, *27*, 779–788. [CrossRef]
37. Azizieh, M.; Dezfuli, M.A.G.; Balak, Z.; Kim, H.S. A novel approach for producing in situ Al-Al_2Cu composite via friction stir processing. *Mater. Res. Express* **2018**, *6*, 036528. [CrossRef]
38. Embury, J.; Lloyd, D.; Ramachandran, T. Strengthening mechanisms in aluminum alloys. In *Treatise on Materials Science & Technology*; Elsevier: Amsterdam, The Netherlands, 1989; pp. 579–601.
39. Saboori, A.; Dadkhah, M.; Fino, P.; Pavese, M. An overview of metal matrix nanocomposites reinforced with graphene nanoplatelets; mechanical, electrical and thermophysical properties. *Metals* **2018**, *8*, 423. [CrossRef]
40. Nazari, M.; Eskandari, H.; Khodabakhshi, F. Production and characterization of an advanced AA6061-Graphene-TiB2 hybrid surface nanocomposite by multi-pass friction stir processing. *Surf. Coat. Technol.* **2019**, *377*, 124914. [CrossRef]
41. American Society of Mechanical Engineers. *BPVC Section IX-Welding, Brazing, and Fusing Qualifications*; ASME: New York, NY, USA, 2023.
42. Elangovan, K.; Balasubramanian, V. Influences of post-weld heat treatment on tensile properties of friction stir-welded AA6061 aluminum alloy joints. *Mater. Charact.* **2008**, *59*, 1168–1177. [CrossRef]
43. Sachinkumar, S.; Narendranath, S.; Chakradhar, D. Microstructure, hardness and tensile properties of friction stir welded aluminum matrix composite reinforced with SiC and fly ash. *Silicon* **2019**, *11*, 2557–2565. [CrossRef]
44. Sharma, C.; Dwivedi, D.K.; Kumar, P. Influence of in-process cooling on tensile behaviour of friction stir welded joints of AA7039. *Mater. Sci. Eng. A* **2012**, *556*, 479–487. [CrossRef]
45. Zhang, Z.; Xiao, B.; Ma, Z. Enhancing mechanical properties of friction stir welded 2219Al-T6 joints at high welding speed through water cooling and post-welding artificial ageing. *Mater. Charact.* **2015**, *106*, 255–265. [CrossRef]
46. Rathinasuriyan, C.; Pavithra, E.; Sankar, R.; Kumar, V.S. Current status and development of submerged friction stir welding: A review. *Int. J. Precis. Eng. Manuf. Green Technol.* **2021**, *8*, 687–701. [CrossRef]